RSC Advances

ROYAL SOCIETY OF CHEMISTRY

www.rsc.org/advances

Journal Name

RSCPublishing

COMMUNICATION

Facile synthesis of zeolite-encapsulated iron oxide nanoparticles as a superior catalyst for phenol oxidation

Cite this: DOI: 10.1039/xoxxoooooox

Received ooth January 2012,
Accepted ooth January 2012

DOI: 10.1039/xoxxoooooox

www.rsc.org/

Lei Luo[a], Chengyi Dai[a], Anfeng Zhang[a], Junhu Wang[b], Min Liu[a], Chunshan Song[ac]* and Xinwen Guo[a]*

Meso-ZSM-5 modified by polyethyleneimine has been found to be an excellent support for iron oxide with improved physicochemical properties of iron oxide particles including size and chemical state. The resulting ZSM-5 encapsulated iron nanoparticles exhibit superior catalytic activity for phenol oxidation.

Advanced oxidation processes (AOPs), as effective methods for destruction of the organic contaminants present in the wastewater, draw much attention nowadays in the wide range of investigations.[1] Owing to their unique catalytic performance, iron-based materials together with hydrogen peroxide constitute important AOPs system.[2] Development of a strategy to control the properties or features of iron-based catalysts including Fe^{3+}/Fe^{2+} ratio and dispersion which determine the catalytic efficiency is of great significance.

Since the iron-based heterogeneous catalyst was first introduced in 1996[3], various molecular sieves including microporous zeolites, mesoporous material (SBA-15[4], MCM-41[5]) and metal organic frameworks (MOFs)[6], have been developed as iron supports. Compared with the latter two supports, zeolite-supported iron shows higher catalytic activity due to its approximate acidity which is beneficial for the adsorption of the organics[7]. However, the supported iron in most cases remains on the outer surface of the zeolite as bulky materials[8] which decrease the iron dispersion. Recently, mesoporous zeolite has been developed as a support to decrease the metal particle size[9]. However, the chemical nature of iron species (e.g. Fe^{3+}/Fe^{2+} ratio) is hardly controlled by conventional impregnation method.

Herein, a facile synthesis strategy was designed for enhancing the dispersion as well as adjusting the chemical state of iron (Fig. 1a). By using mesoporous zeolite modified with polyethyleneimine (PEI) as a support, iron particle size was decreased through amine immobilization which prevents the iron precursor migrating during thermal treatment. At the same time, the thermal decomposition of PEI is accompanied with a redox process leading to the transition from Fe^{3+} to Fe^{2+}, which shows excellent performance in phenol degradation[10].

Besides PEI/meso-ZSM-5 composite, two other supports were used in this work as a benchmark, including micro-ZSM-5, meso-ZSM-5, which were prepared through hydrothermal synthesis[11] and alkaline treatment[12], respectively. Through incipient wetness impregnation method using aqueous solutions of iron nitrates ($Fe(NO_3)_3$•$9H_2O$), three catalysts with 5 wt% Fe loading were prepared. The as-prepared catalysts were coded by P, AT, and N600, all went through the same thermal treatment at 873 K for 3 h in N_2. Fig. 1b shows the STEM image of sample P, it can be seen that iron particle with ca. 40 nm on the surface of ZSM-5. When using meso-ZSM-5 as a support, iron particle size clearly decreased (Fig. 1c) which attributed to the increased external surface area (Table S1). Upon using PEI modified meso-ZSM-5 as a support; the iron particle size was further decreased, as can be seen from Figs. 1d, and 1e.

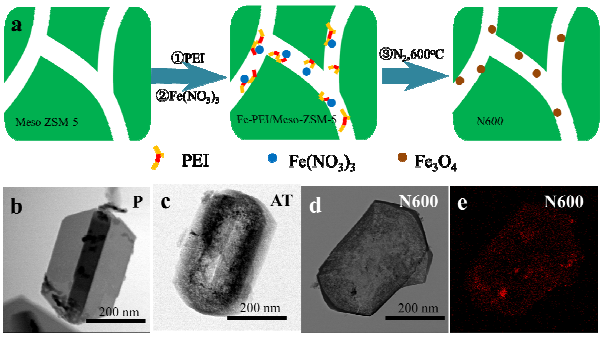

Fig. 1 (a) Process of N600 preparation, (b, c, d) STEM images of P, AT and N600, respectively, (e) TEM-EDS image of N600. Red color represents iron.

The XRD patterns of P, AT and N600 are shown in Fig. S1 which clearly exhibit MFI diffraction peaks of ZSM-5. The diffraction peaks at around 33.2° and 35.7° 2θ of sample P indicate the existence of α-Fe_2O_3, the particle size calculated from surface [104] and surface [110] by the Scherrer equation is 22.2 nm and 40.4 nm, respectively. While sample AT and N600 show the absence of those diffraction peaks which point to the highly dispersed iron, in line with the STEM images.

Fig. S2 shows the Ar adsorption/desorption isotherms of those catalysts. Compared with sample P, the isotherms of AT and N600 exhibit a steep increase from P/P_0=0.6 to P/P_0=1, which is the evidence of the presence of mesopores. The external surface area of AT and N600 are 240 and 222 m^2/g, respectively, which is almost twice of P (125 m^2/g). Furthermore, AT and N600 possess mesopore of around 10 nm (inset of Fig. S2).

To investigate the reducibility of sample P, AT, and N600, H_2-TPR experiments were conducted (shown in Fig. S3). For sample P, the H_2 consumption peaks correspond to the combined Fe^{3+} and (or) α-Fe_2O_3 nanoparticles to $Fe^{(3-\delta)+}$ (α1) with intermediate valence as that in Fe_3O_4 and then to Fe^{2+} (α2). At higher temperature, the peaks represent partial reduction of Fe^{2+} to Fe^0 (α3, α4).[13] Sample N600 shows the decrease of H_2 consumption peak above 773 K and shift to a lower temperature, which is attributed to the strong interaction between iron oxide nanoparticles and the support. On the other hand, compared with AT, the H_2 consumption of N600 decreased, which can be attributed to previously transition from Fe_2O_3 to Fe_3O_4 during the preparation of thermal treatment.

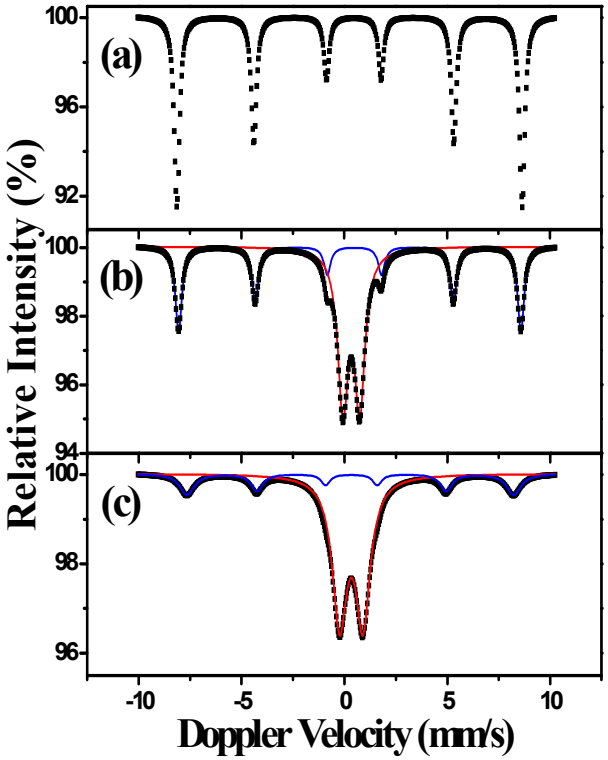

Fig. 2 ^{57}Fe Mossbauer spectroscopy of (a) P, (b) AT, (c) N600.

The Fe 2p XPS spectra of P, AT, and N600 are shown in Fig. S4. It clearly shows that sample P has higher intensity of Fe 2p, while sample AT shows weakest Fe 2p intensity. Considering that the detection depth of XPS is limited to about 2 nm, the content of iron located on the outer surface of sample AT is much lower than sample P and N600. From the deconvolution of the Fe 2p XPS spectra of Fe $2P_{3/2}$, peaks which centered at 710.8 eV and 708.5 eV are attributed to Fe^{3+} and Fe^{2+}, respectively. For sample P, only one distinct peak centered at 710.8 eV was observed, indicating that iron in sample P is present only as Fe^{3+} and, therefore, the iron oxide species is Fe_2O_3.[14] In the case of sample N600, two distinct peaks are present indicating the coexistence of Fe^{2+} and Fe^{3+}, confirming the existence of Fe_3O_4 species.

To further investigate the metal oxide species of the three samples in our work, ^{57}Fe Mossbauer spectra of sample P, AT and N600 are shown in Fig. 2, with the hyperfine interaction parameters summarized in Table S2. The peak type can reflect the particle size by determining whether the iron oxide particle is superparamagnetic or not. When the particle size of the iron oxide is below a critical point, super paramagnetic phenomenon converts the peak to a sextet. Contrarily, above the critical point the peak presents as a doublet. On the other hand, the 57Fe Mossbauer parameter can reflect the metal species according to the literature[16]. In the case of sample P, the Mossbauer peak of IS = 0.38 mm/s and QS = -0.21 mm/s are in agreement with those values for α-Fe_2O_3 in the form of a sextet.[15] For sample AT, peaks of α-Fe_2O_3 in the form of both a sextet and a doublet[15] are observed simultaneously with the sextet relative intensity (RI) decreasing from 100 % to 41.2 %. The doublet， with ^{57}Fe Mossbauer parameters of IS = 0.34 mm/s and QS = 0.82 mm/s, accounted for about 58.8%. This change from sextet to doublet is due to the decrease in particle size, which has been confirmed by STEM and XRD. As for sample N600, the particle size is further minimized because the RI of the sextet further decreased to 22.6% and ^{57}Fe Mossbauer parameters of IS = 0.31 mm/s and QS = -0.05 mm/s are attributed to Fe_3O_4.[16] This indicates that PEI did have a positive impact on minimizing the particle size as well as reducing the iron oxide.

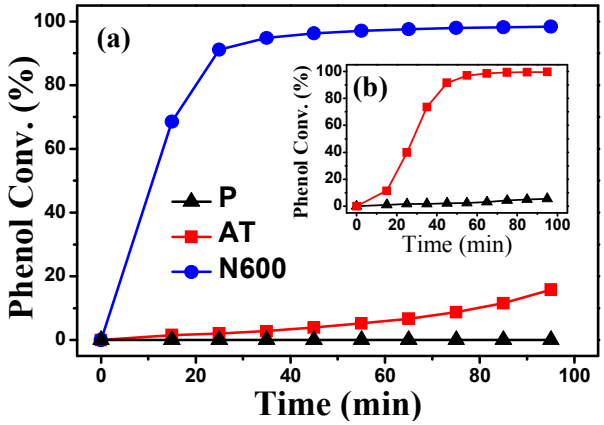

Fig. 3 The phenol degradation catalyzed by samples P, AT, and N600. Reaction conditions: $n(H_2O_2)$:n(phenol)=14, C(phenol)=1g/L, $C(H_2O_2)$=0.69 M, pH=6.2, Temperature (a) 308 K, (b) 338 K.

The initial catalytic activity of the prepared samples was evaluated for phenol degradation reaction. As shown in Fig. 3, the initial catalytic activity of P and AT was lower than that of N600, which is attributed to the increased content of Fe^{2+} as well as the minimized nanoparticle size. Sample AT exhibited a smaller iron oxide size compared with P. The reaction temperature has a great influence on the catalytic oxidation. As shown in the inset of Fig. 3, when the temperature was increased from 308 to 338 K, the advantages of the minimized particle size begin to appear, where sample AT shows a much higher catalytic activity than sample P. It is the minimized particle size that made the catalytic difference of P and AT, and the reduction of iron by PEI led to the great catalytic difference of N600 at lower temperature. Meso-ZSM-5 has the effect on minimizing the particle size of iron oxide, meanwhile, the

presence of PEI can enhance this effect by preventing $Fe(NO_3)_3$ from migrating as well as reducing of Fe^{3+} during the thermal treatment preparation.

In summary, PEI has been successfully used for the first time to fabricate catalyst with superior activity in phenol oxidation. By using meso-ZSM-5 modified with PEI as a support, iron particle size has been decreased through amine immobilization which prevented the iron precursor migrating during thermal treatment. At the same time, the thermal decomposition of PEI is accompanied with a redox process leading to the transition from Fe^{3+} to Fe^{2+}, which is good for the enhancement of catalytic property in phenol oxidation.

Our work provides a guide for improved impregnation process using low melting point metal precursor with minimized particle size and the facile preparation of transition metal oxide with adjustable physicochemical state.

Acknowledgements

This work was supported by the State Key Program of National Natural Science Foundation of China (grant no. 21236008).

Notes and references

[a] State Key Laboratory of Fine Chemicals, PSU-DUT Joint Center for Energy Research, School of Chemical Engineering, Dalian University of Technology, Dalian 116024, P. R. China. E-mail: guoxw@dlut.edu.cn; Fax: +86-0411-84986134; Tel: +86-0411-84986133

[b] Mossbauer Effect Data Center, Dalian Institute of Chemical Physics, Chinese Academy of Sciences, Dalian, 116023, China

[c] EMS Energy Institute, PSU-DUT Joint Center for Energy Research and Department of Energy & Mineral Engineering, Pennsylvania State University, University Park, Pennsylvania 16802, USA, E-mail: csong@psu.edu; Fax: +1-814-865-3573; Tel: +1-814-863-4466

† Electronic Supplementary Information (ESI) available: [synthesis of P, AT and N600, catalyst performance, Ar adsorption and desorption isotherms, XRD, XPS].

1 (a) F. C. Moreira, S. Garcia-Segura, R. A. R. Boaventura, E. Brillas and V. J. P. Vilar, Appl. Catal., B, 2014, 160-161, 492-505. (b) M. Antonopoulou, E. Evgenidou, D. Lambropoulou and I. Konstantinou, Water Res., 2014, 53, 215-234. (c) A. D. Bokare and W. Choi, J. Hazard. Mater., 2014, 275, 121-135.

2 (a) J. V. Coelho, M. S. Guedes, R. G. Prado, J. Tronto, J. D. Ardisson, M. C. Pereira and L. C. A. Oliveira, Appl. Catal., B, 2014, 144, 792-799. (b) S. Fukuchi, R. Nishimoto, M. Fukushima and Q. Zhu, Appl. Catal., B, 2014, 147, 411-419. (c) R. Prihod Ko, I. Stolyarova, G. Gündüz, O. Taran, S. Yashnik, V. Parmon and V. Goncharuk, Appl. Catal., B, 2011, 104, 201-210.

3 K. Fajerwerg and H. Debellefontaine, Appl. Catal., B, 1996, 10, L229-L235.

4 (a) C. H. Christensen, I. Schmidt, A. Carlsson, K. Johannsen and K. Herbst, J. Am. Chem. Soc., 2005, 127, 8098-8102. (b) A. Y. Khodakov, A. Griboval-Constant, R. Bechara and V. L. Zholobenko, J Catal., 2002, 206, 230-241. (c) H. Song, R. M. Rioux, J. D. Hoefelmeyer, R. Komor, K. Niesz, M. Grass, P. Yang and G. A. Somorjai, J. Am. Chem. Soc., 2006, 128, 3027-3037. (d) R. M. Rioux, H. Song, J. D. Hoefelmeyer, P. Yang and G. A. Somorjai, J. Phy. Chem. B, 2005, 109, 2192-2202. (e) F. Su, J. Zeng, X. Bao, Y. Yu, J. Y. Lee and X. S. Zhao, Chem. Mater., 2005, 17, 3960-3967. (f) X. LI, W. JI, J. ZHAO, S. WANG and C. AU, J. Catal., 2005, 236, 181-189. (g) L. Chmielarz, P. Kuśtrowski, R. Dziembaj, P. Cool and E. F. Vansant, Appl. Catal., B, 2006, 62, 369-380. (h) F. Martínez, G. Calleja, J. A. Melero and R. Molina, Appl. Catal., B, 2007, 70, 452-460. (i) M. Mureddu, I. Ferino, A. Musinu, A. Ardu, E. Rombi, M. G. Cutrufello, P. Deiana, M. Fantauzzi and C. Cannas, J. Mater. Chem., A, 2014, 2, 19396-19406.

5 (a) J. F. Bengoa, M. V. Cagnoli, N. G. Gallegos, A. M. Alvarez, L. V. Mogni, M. S. Moreno and S. G. Marchetti, Microporous Mesoporous Mater., 2005, 84, 153-160. (b) M. Xia, M. Long, Y. Yang, C. Chen, W. Cai and B. Zhou, Appl. Catal., B, 2011, 110, 118-125. (c) A. I. Carrillo, E. Serrano, R. Luque and J. García-Martínez, Appl. Catal., A, 2013, 453, 383-390.

6 N. A. Khan and S. H. Jhung, J. Hazard. Mater., 2012, 237-238, 180-185.

7 (a) K. Na, C. Jo, J. Kim, K. Cho, J. Jung, Y. Seo, R. J. Messinger, B. F. Chmelka and R. Ryoo, Science, 2011, 333, 328-332. (b) X. Zhang, W. Yu, Y. Qin, S. Dong, T. Pei, L. Wang, L. Song. Acta Phys. -Chim. Sin. 2013, 29(06), 1273-1280.

8 (a) C. Knapp, A. Obuchi, J. O. Uchisawa, S. Kushiyama and P. Avila, Microporous Mesoporous Mater., 1999, 31, 23-31. (b) C. H. Christensen, I. Schmidt, A. Carlsson, K. Johannsen and K. Herbst, J. Am. Chem. Soc., 2005, 127, 8098-8102.

9 (a) C. Dai, A. Zhang, L. Li, K. Hou, F. Ding, J. Li, D. Mu, C. Song, M. Liu and X. Guo, Chem. Mater., 2013, 25, 4197-4205. (c) D. Verboekend, R. Caicedo-Realpe, A. Bonilla, M. Santiago and J. Pérez-Ramírez, Chem. Mater., 2010, 22, 4679-4689. (d) J. Mielby, J. O. Abildstrøm, F. Wang, T. Kasama, C. Weidenthaler and S. Kegnaes, Angew. Chem. Int. Ed., 2014, n/a-n/a.

10 (a) R. Costa, M. Lelis, L. Oliveira, J. Fabris, J. Ardisson, R. Rios, C. Silva and R. Lago, J. Hazard. Mater., 2006, 129, 171-178. (b) R. C. C. Costa, F. C. C. Moura, J. D. Ardisson, J. D. Fabris and R. M. Lago, Appl. Catal. B, 2008, 83, 131-139.

11 M. M. Forde, R. D. Armstrong, C. Hammond, Q. He, R. L. Jenkins, S. A. Kondrat, N. Dimitratos, J. A. Lopez-Sanchez, S. H. Taylor, D. Willock, C. J. Kiely and G. J. Hutchings, J. Am. Chem. Soc., 2013, 135, 11087-11099.

12 (a) D. Verboekend, G. Vilé and J. Pérez-Ramírez, Adv. Funct. Mater., 2012, 22, 916-928. (b) K. Möller and T. Bein, Chem. Soc. Rev., 2013, 42, 3689. (c) M. Milina, S. Mitchell, P. Crivelli, D. Cooke and J. Pérez-Ramírez, Nat. Commun., 2014.

13 F. Liu, H. He, C. Zhang, Z. Feng, L. Zheng, Y. Xie and T. Hu, Appl. Catal., B, 2010, 96, 408-420.

14 (a) J. Gao, X. Ran, C. Shi, H. Cheng, T. Cheng and Y. Su, Nanoscale, 2013, 5, 7026. (b) T. Yamashita and P. Hayes, Appl. Surf. Sci., 2008, 254, 2441-2449.

15 R. Zboril, M. Mashlan and D. Petridis, Chem. Mater., 2002, 14, 969-982.

16 K. Woo, J. Hong, S. Choi, H. Lee, J. Ahn, C. S. Kim and S. W. Lee, Chem. Mater., 2004, 16, 2814-2818.